Journal of Materials Chemistry C

Accepted Manuscript

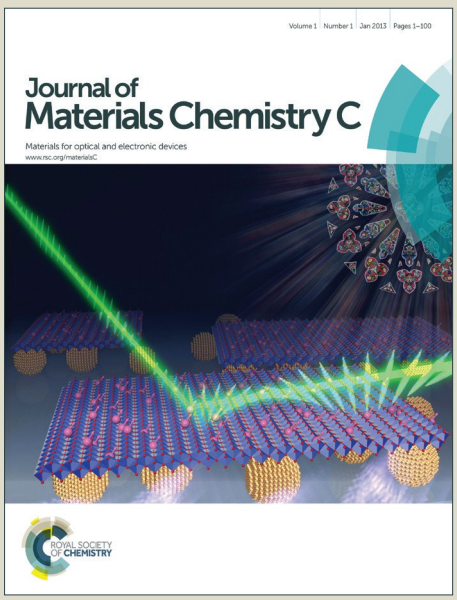

ROYAL SOCIETY OF CHEMISTRY

www.rsc.org/materialsC

Journal of
Materials Chemistry C

COMMUNICATION

A fluorescent and halochromic indolizine switch†

Yang Zhang, Jaume Garcia-Amorós, Burjor Captain and Françisco M. Raymo*

Received 14th October 2015,
Accepted #

DOI: 10.1039/#

www.rsc.org/MaterialsC

An indolizine heterocycle switches from a nonemissive to an emissive form upon protonation. The co-entrapment of this molecular switch and a photoacid generator in polymer films allows the imprinting of fluorescent patterns in the resulting materials. These operating principles permit the writing and reading of information under optical control.

The photochemical transformation of a nonemissive reactant into a fluorescent product allows the activation of fluorescence under optical control.[1–5] In turn, the sequential acquisition of fluorescence images, after activation, can be exploited to track the diffusion of species in real time[6,7] and to visualize specimens at the nanoscale.[8,9] These promising applications, however, require photoactivatable fluorophores with optimal photochemical and photophysical properties. As a result, significant research efforts are currently directed at the identification of viable structural designs to photoswitch efficiently the fluorescence of organic chromophores from off to on with large contrast and high brightness. Generally, either the photoinduced cleavage of a protecting group or a photochromic transformation is engineered to suppress a quenching pathway and permit the radiative deactivation of a given chromophore upon excitation. Alternatively, the very same photochemical processes can be adapted to alter the ability of the chromophore to absorb and enable the selective excitation of the product. In all instances, the overall result is the activation of fluorescence after a photoinduced unimolecular reaction.

Certain organic chromophores alter reversibly their ability to absorb radiations in the visible region of the electromagnetic spectrum upon acidification.[10] This phenomenon, termed halochromism,[11] causes drastic changes in color and is behind the operating principles of pH indicators[12] and smart inks.[13–15] Generally, the protonation of an appropriate auxochrome shifts bathochromically the main absorption of the chromophore and, therefore, alters the color of the sample. This spectral change allows also the selective excitation of the protonated form at an appropriate wavelength with concomitant emission, if the excited chromophoric component can deactivate radiatively. As a result, some halochromic molecular switches can be employed to sense pH with fluorescence measurements.[16,17]

Halochromic molecular switches can be operated in conjunction with photoacid generators under the influence of optical stimulations.[18] Excitation of the latter species results in the photoinduced release of acid, which can then protonate the former. If the protonated form of the halochromic switch is emissive, then excitation also of this component generates fluorescence. In fact, we developed viable mechanisms to photoactivate fluorescence on the basis of these bimolecular processes and demonstrated that these strategies can be exploited to monitor proton diffusion across polymer films in real time and image nanoparticles with spatial resolution at the nanometer level.

Our halochromic fluorophores generally rely on the opening of a 2*H*,3*H*-benzo[1,3]oxazine ring upon acidification.[18] This heterocyclic system can be prepared from 2,3,3-trimethyl-3*H*-indole in one synthetic step and then condensed to a fluorescent chromophore in a second. In order to regulate the spectral response of the final product, we envisaged the possibility of introducing electron withdrawing substituents on the indole precursor. Specifically, we attempted to adapt a literature procedure[19] for the attachment of 1,2,2-tricyanoethyn-1-yl substituents to heteroaromatic compounds. We isolated instead an indolizine heterocycle and, to our surprise, found that this molecule is a fluorescent halochromic switch. Here, we report the synthesis and structural characterization of this compound, together with its electrochemical and photophysical properties, and demonstrate that this halochromic switch can be exploited to imprint fluorescent patterns in polymer films.

Heating an equimolar *N*,*N*-dimethylformamide (DMF) solution of 2,3,3-trimethyl-3*H*-indole and tetracyanoethylene (TCNE) at 80 °C for one hour, under an atmosphere of argon, produced **1** (Fig. 1) in a yield of 62%. Single crystals of the product, suitable for X-ray diffraction analysis‡ (Table S1), could be obtained after the slow evaporation of an ethyl acetate solution of the compound. The resulting structure (Fig. 2a) confirms the formation of an indolizine heterocycle with two cyano substituents and one imino group. Furthermore, it shows that the molecule has crystallographic mirror symmetry with these three functional groups and the three fused rings in a coplanar arrangement.

Laboratory for Molecular Photonics, Department of Chemistry, University of
**Email: fraymo@miami.edu*
† Electronic Supplementary Information (ESI) available: experimental procedures, crystallographic data. See DOI: 10.1039/#

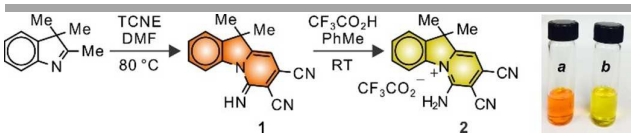

Fig. 1. Synthesis of **1** and its conversion into **2** upon acidification together with a picture of PhMe solutions of **1** (***a***) and **2** (***b***).

In agreement with the crystal structure, the electrospray ionization mass spectrum (ESIMS) reveals a peak at 261 for $[M + H]^+$. The infrared (IR) absorption spectrum confirms further the presence of cyano and imino groups, showing peaks at 2218 and 3306 cm^{-1} for [C≡N] and [N–H] stretching vibrations respectively. Similarly, the ^1H nuclear magnetic resonance (NMR) spectrum (Fig. 3a) shows resonances for the five heterotopic protons (H^A–H^E) of the fused ring system, together with a singlet for the imino proton (H^F), between 6 and 9 ppm. Additionally, it reveals a singlet for the six homotopic methyl protons at 1.55 ppm. Finally, the ^{13}C NMR spectrum shows resonances for the 15 heterotopic carbon atoms incorporated within the structure of **1**.

Treatment of a toluene solution of **1** with CF_3CO_2H (5 eq.) generates **2** (Fig. 1) and causes a change in color from orange (Fig. 1a) to yellow (Fig. 1b). After the slow evaporation of the solvent from the acidified solution, single crystals of the product, suitable for X-ray diffraction analysis[¶] (Table S1), could be obtained. The resulting structure (Fig. 2b) confirms the conversion of the imino group of **1** into the primary amine[§] of **2** with an elongation of the [C4–N4] distance from 1.28 to 1.32 Å. Similarly, the adjacent [C4–N3] bond shortens from 1.40 to 1.36 Å with the conversion of **1** into **2**, but the associated six-membered ring retains bond alternation with minimal changes in the lengths of the other five bonds. Furthermore, the co-planar arrangement of the three fused rings of **1** is lost with the formation of **2**. In the latter structure, the two six-membered rings are twisted by *ca.* 13° around the [C–N] bond connecting them.

The conversion of **1** into **2** shifts the doublet associated with H^A from 9.01 to 8.16 ppm in the ^1H NMR spectrum (Fig. 3a–f). In **1**, an intramolecular hydrogen bonding interaction between H^A and the imino nitrogen atom is responsible for the relatively high chemical shift of this proton. In **2**, the lone pair of the amino nitrogen atom is shared with the adjacent pyridinium ring and cannot maintain the hydrogen bond with H^A. Therefore, the chemical shift of the corresponding resonance decreases significantly. A shift in the opposite direction is observed instead for the singlet associated with H^E, which moves from 6.07 to 7.78 ppm (Fig. 3a–f). In fact, the conversion of the imino group of **1** into the primary amine of **2** imposes cationic character on the associated heterocyclic ring

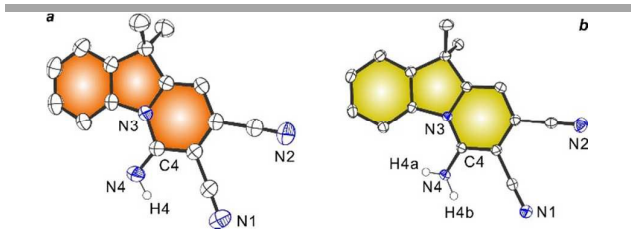

Fig. 2 ORTEP representations of the crystal structures of **1** (***a***) and **2** (***b***) showing thermal ellipsoids at the 50% probability level.

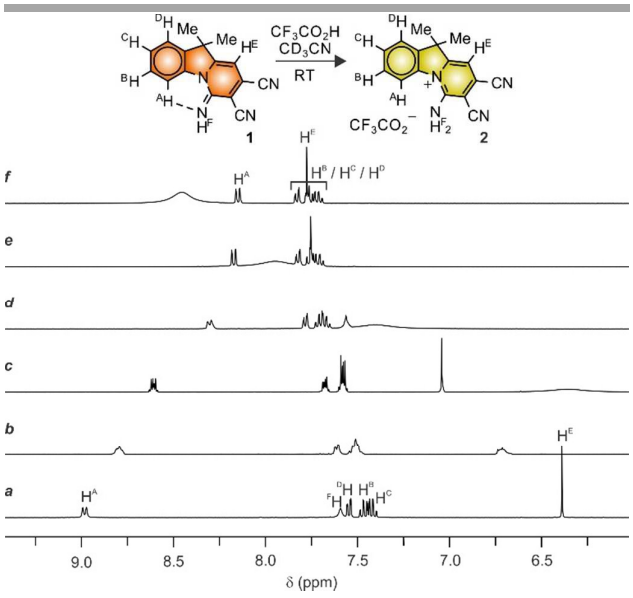

Fig. 3 ^1H NMR spectra (400 MHz, CD_3CN) of **1** before (***a***) and after the addition of 0.5 (***b***), 1 (***c***), 2 (***d***), 3 (***e***) and 5 eq. (***f***) of CF_3CO_2H.

and increases the chemical shift of H^E.

The ultraviolet/visible (UV/VIS) absorption spectrum (Fig. 4a) of **1** shows a band at 477 nm with a molar absorption coefficient of 9.5 mM^{-1} cm^{-1}. Illumination of the sample at 370 nm does not produce any detectable emission (Fig. 4i). Upon addition of increasing amounts of CF_3CO_2H, the absorption at 477 nm decreases (Fig. 4b–h) with the concomitant growth of a new band at 398 nm, in agreement with the conversion of **1** into **2**. Excitation within the developing absorption results in intense emission at 470 nm (Fig. 4j–p) with a fluorescence quantum yield of 0.27. Thus, the halochromic transformation of **1** into **2** can be exploited to activate fluorescence efficiently with excellent contrast. Furthermore, the spectral changes can be fully reversed with the addition of increasing amounts of Bu_4NOH. Under these conditions, **2** switches to **1** and the absorption band at 477 nm grows back to the original value (Fig. 4g and 4q–t) with a concomitant decrease in absorbance at 398 nm and the suppression of the emission intensity (Fig. 4o and 4u–y).

The different electronic structure of **1** and **2**, evident from the spectroscopic measurements, is reflected also in their voltammetric response. The cyclic voltammogram of **1** (Fig. 5a) shows an irreversible oxidation at +1.27 V and a reversible reduction with half-wave potential of –1.35 V. Upon addition of CF_3CO_2H in excess, **1** switches to **2** and the wave for the oxidation process disappears (Fig. 5b). Additionally, the formation of **2** shifts the half-wave potential for the reduction process to –0.65 V (Fig. 5c). These changes are consistent with the cationic character of **2**, which facilitates reduction and prevents oxidation. Furthermore, the cyclic voltammogram of **2** shows also a second irreversible reduction process at –1.07 V (Fig. 5c).

The halochromic transformation of **1** into **2** can be induced under the influence of optical simulations with the aid of a photoacid generator. In particular, the illumination of **3** (Fig. 6) at an appropriate wavelength produces **4** with the concomitant release of hydrobromic acid.[18] In turn, the

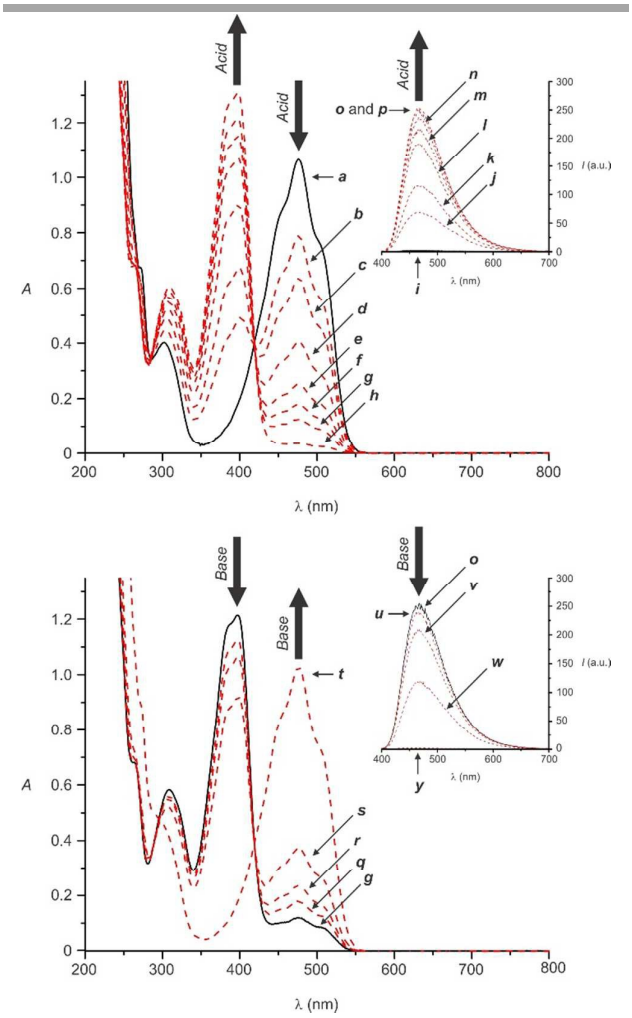

Fig. 4 Absorption and emission (λ_{Ex} = 370 nm) spectra of **1** (0.1 mM, MeCN) before (***a*** and ***i***) and after the addition of 1 (***b*** and ***j***), 2 (***c*** and ***k***), 4 (***d*** and ***l***), 6 (***e*** and ***m***), 8 (***f*** and ***n***), 10 (***g*** and ***o***) and 20 eq. (***h*** and ***p***) of CF_3CO_2H. Absorption and emission (λ_{Ex} = 370 nm) spectra of **1** (0.1 mM, MeCN) and CF_3CO_2H (10 eq.) before (***g*** and ***o***) and after the addition of 1 (***q*** and ***u***), 2 (***r*** and ***v***), 5 (***s*** and ***w***) and 10 eq. (***t*** and ***y***) of Bu_4NOH.

photogenerated acid can be exploited to switch **1** into **2** and allow the activation of the fluorescence of the latter species. This mechanism for fluorescence activation permits the writing of emissive patterns in poly(butyl methacrylate) (PBMA) films doped with a mixture of **1** and the photoacid generator. Specifically, a fluorescence image (Fig. 6a) of a doped PBMA film, recorded after illuminating a defined region at 405 nm, shows intense emission exclusively in the irradiated area. Indeed, the illuminating beam encourages the local release of acid with the conversion of the nonemissive reactant into the fluorescent product. The formation of the latter can then be detected by recording its intense emission between 420 and 500 nm. Furthermore, an image recorded after 60 min (Fig. 6b) clearly reveals that the shape of the fluorescent area and its emission intensity remain unchanged. In fact, fluorescent patterns with microscaled resolution (Fig. 6c) and even text (Fig. 6d) can be imprinted in the photoresponsive material.

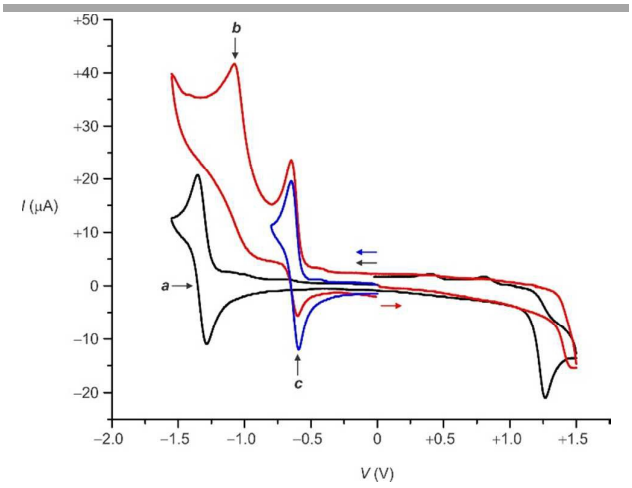

Fig. 5 Cyclic voltammogram [1 mM, MeCN, Bu_4NPF_6 (0.1 M), V *vs.* Ag/Ag^+ (1 mM $AgNO_3$ in MeCN), 100 mV s^{-1}] of **1** before (***a***) and after (***b*** and ***c***) the addition of CF_3CO_2H (20 eq.).

Thus, these operating principles offer the opportunity to write and read information with light on the basis of the photoinduced transfer of protons between complementary molecular components.

Our results demonstrate that a substituted indolizine heterocycle can be prepared efficiently in a single synthetic step from readily available precursors. Protonation of the imino group of this compound alters drastically the electronic structure of the heterocyclic ring system to impose a pronounced hypsochromic shift in absorption and allow radiative deactivation after excitation. As a result, this halochromic transformation is accompanied by the activation of bright fluorescence with excellent contrast. The very same

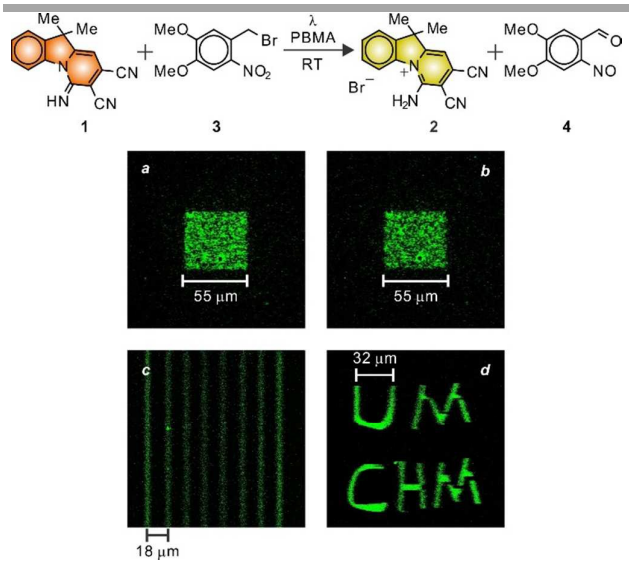

Fig. 6 Confocal laser-scanning fluorescence images (λ_{Ex} = 405 nm, λ_{Ex} = 420–500 nm) of PBMA films, doped with **1** (5% w/w) and **3** (5% w/w), recorded immediately (***a***, ***c*** and ***d***) and 60 min (***b***) after illumination (405 nm, 0.1 mW, 20 s) of defined areas within the imaging field.

process can be induced with the assistance of a photoacid generator, under the influence of optical stimulations. The co-entrapment of halochromic switch and photoacid generator within a polymer film permits the activation of the fluorescence of the former upon excitation of the latter. These operating principles translate into photoresponsive materials that allow the optical writing and reading of patterns with spatial control at the micrometer level.

Acknowledgements

The National Science Foundation (CHE-1049860) is acknowledged for financial support. JGA is grateful for *Beatriu de Pinós* post-doctoral grants (2011 BP-A-00270 and 2011 BP-A2 00016) from the *Generalitat de Catalunya* (Spain).

Notes and references

‡ Crystal data for **1**: $C_{16}H_{12}N_4$, M_r = 260.30, orthorombic, space group *Pnma*, *a* = 13.0779(6) Å, *b* = 6.7374(3) Å, *c* = 14.8646(7) Å, *V* = 1309.74(10) Å^3, *Z* = 4, *T* = 296 K, Mo K_α = 0.71073 Å. GOF = 1.052, No. Parameters = 123, $2\Theta_{max}$ = 54°. The final *R1*(F^2) was 0.0377 for 1368 reflections I>2σ(I). CCDC No. 1426007.

¶ Crystal data for **2**: $C_{20}H_{14}N_4F_6O_4$, M_r = 488.35, monoclinic, space group $P2_1/n$, *a* = 8.6010(4) Å, *b* = 21.0213(10) Å, *c* = 11.9369(6) Å, β = 104.717(1) °*V* = 2087.43(17) Å^3, *Z* = 4, *T* = 100 K, Mo K_α = 0.71073 Å. GOF = 1.020, No. Parameters = 318, $2\Theta_{max}$ = 56°. The final *R1*(F^2) was 0.0381 for 4118 reflections I>2σ(I). CCDC No. 1430926.

§ An amino group is proposed in **2** because of the successful location and refinement of two hydrogen atoms (H4a and H4b in Fig. 2b) on N4 in the structural analysis.

1 L. M. Wysocki and L. D. Lavis, *Curr. Op. Chem. Biol.*, 2011, **15**, 752–759.
2 D. Puliti, D. Warther, C. Orange, A. Specht and M. Goeldner, *Bioorg. Med. Chem.*, 2011, **19**, 1023–1029.
3 W.-H. Li and W.-H. Zheng, *Photochem. Photobiol. Sci.*, 2012, **11**, 460–471.
4 P. Klán, T. Šolomek, C. G. Bochet, A. Blanc, R. Givens, M. Rubina, V. Popik, A. Kostikov and J. Wirz, *Chem. Rev.*, 2013, **113**, 119−191.
5 F. M. Raymo, *Phys. Chem. Chem. Phys.,* 2013, **15**, 14840−14850.
6 Y. Xu, T. J. Melia and D. T. Toomre, *Curr. Op. Chem. Biol.*, 2011, **15**, 822–830.
7 F. M. Raymo, *ISRN Phys. Chem.*, 2012, 619251-1–15.
8 S. van de Linde, M. Heilemann and M. Sauer, *Ann. Rev. Phys. Chem.*, 2012, **63**, 519–540.
9 T. Ha and P. Tinnefeld, *Ann. Rev. Phys. Chem.*, 2012, **63**, 595–617.
10 B. L. Feringa and W. L. Brown, *Molecular Switches*, Wiley-VCH, Weinheim, 2011.
11 P. Muller, *Pure Appl. Chem.*, 1994, **66**, 1077–1184.
12 J. G. Speight, *Lange's Handbook of Chemistry*, McGraw-Hill, New York, 2005.
13 T. Horiguchi, Y. Koshiba, Y. Ueda, C. Origuchi and K. Tsutsui, *Thin Solid Films*, 2008, **516**, 2591–2594.
14 L. Sheng, M. Li, S. Zhu, H. Li, G. Xi, Y. G. Li, Y. Wang, Q. Li, S. Liang, K. Zhong and S. X.-A. Zhang *Nat. Commun.*, 2014, **5**, 3044-1–8.
15 J. Garcia-Amorós, S. Swaminathan, F. M. Raymo, *Dyes Pigments*, 2014, **106**, 71–73.
16 J. Han and K. Burgess, *Chem. Rev.*, 2010, **110**, 2709–2728.
17 R. Wang, C. Yu, F. Yu and L. Chen, *Trac-Trend Anal. Chem.*, 2010, **29**, 1004–1013.
18 (a) S. Swaminathan, M. Petriella, E. Deniz, J. Cusido, J. D. Baker, M. L. Bossi and F. M. Raymo, *J. Phys. Chem. A*, 2012, **116**, 9928−9933. (b) M. Petriella, E. Deniz, S. Swaminathan, M. J. Roberti, F. M. Raymo and M. L. Bossi, *Photochem. Photobiol.*, 2013, **89**, 1391–1398.
19 S. Banerjee, F. Ali, P. K. Nayak and N. Agarwal, *Thin Solid Films*, 2012, **520**, 2644–2650.

Graphical Abstract

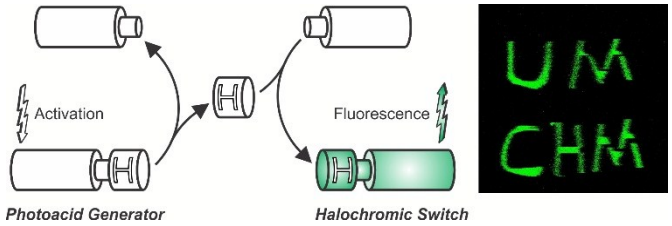

Proton transfer from a photoacid generator to a halochromic molecular switch within a polymer film permits the imprinting of fluorescent patterns under the influence of optical stimulations